THE JOURNAL OF BIOLOGICAL CHEMISTRY
Vol. 278, No. 42, Issue of October 17, pp. 40842–40850, 2003
Printed in U.S.A.

Disruption of *Cg*-Ppm1, a Polyprenyl Monophosphomannose Synthase, and the Generation of Lipoglycan-less Mutants in *Corynebacterium glutamicum**

Received for publication, July 23, 2003, and in revised form, August 5, 2003
Published, JBC Papers in Press, August 6, 2003, DOI 10.1074/jbc.M307988200

Kevin J. C. Gibson‡, Lothar Eggeling§, William N. Maughan‡, Karin Krumbach§, Sudagar S. Gurcha‡, Jérôme Nigou¶, Germain Puzo¶, Hermann Sahm§, and Gurdyal S. Besra‡‖

From the ‡School of Biosciences, University of Birmingham, Edgbaston, Birmingham B15 2TT, United Kingdom, the §Institute for Biotechnologie 1, Research Centre Juelich, D-52425 Juelich, Germany, and the ¶Department of Molecular Mechanisms of Mycobacterial Infections, Institut de Pharmacologie et de Biologie Structurale, CNRS, UMR 5089, 205 route de Narbonne, 31077 Toulouse cedex 4, France

The glycosyl donor, polyprenyl monophosphomannose (PPM), has been shown to be involved in the biosynthesis of the mycobacterial lipoglycans: lipomannan and lipoarabinomannan. The mycobacterial PPM synthase (*Mt-ppm1*) catalyzes the transfer of mannose from GDP-mannose to polyprenyl phosphates. Based on sequence homology to *Mt-ppm1*, we have identified the PPM synthase from *Corynebacterium glutamicum*. In the present study, we demonstrate that the corynebacterial synthase is composed of two distinct domains; a catalytic domain (*Cg-ppm1*) and a membrane domain (*Cg-ppm2*). Through the inactivation of *Cg-ppm1*, we observed a complex phenotype that included altered cell growth rate and inability to synthesize PPM molecules and lipoglycans. When *Cg-ppm2* was deleted, no observable phenotype was noted, indicating the clear organization of the two domains. The complementation of the inactivated *Cg-ppm1* strain with the corresponding mycobacterial enzyme (*Mt*-Ppm1/D2) led to the restoration of a wild type phenotype. The present study illustrates, for the first time, the generation of a lipoglycan-less mutant based on a molecular strategy in a member of the Corynebacterianeae family. Lipoglycans are important immunomodulatory molecules involved in determining the outcome of infection, and so the generation of defined mutants and their subsequent immunological characterization is timely.

Corynebacterial strains are widely distributed throughout nature and represent an important branch of the Actinomycetales family. The human pathogen *Corynebacterium diphtheriae* is the causal agent of diphtheria, and serious economic losses occur from the infection of animals by corynebacterial strains, such as *Corynebacterium pseudotuberculosis* and *Corynebacterium matruchotti* (2, 3). In addition, *Corynebacterium glutamicum* is of industrial importance producing large quantities of amino acids worldwide (4). Corynebacteria belong to a suprageneric actinomycete taxon termed the Corynebacterianeae (5), which includes mycobacteria, rhodococci, nocardiae, and other closely related genera. Therefore, it is of no surprise to find that corynebacteria and mycobacteria share a similar cell envelope ultrastructure, which comprises a core mycolyl-arabinogalactan peptidoglycan complex, termed mAGP (6, 7).

An important class of components, found within the cell envelope, are the biosynthetically related glycolipids, phosphatidyl-*myo*-inositol mannosides (PIMs),[1,2] and lipoglycans, termed lipomannan (LM) and lipoarabinomannan (LAM). These glycolipids and lipoglycans are present within the cell envelope of both mycobacteria (8) and corynebacteria (7, 9). The basic structural features of mycobacterial LAM are well described elsewhere and reveal that LAM possess an amphipathic tripartite structure (10–13). The two common domains include a mannosyl-phosphatidyl-*myo*-inositol anchor (MPI), with a polysaccharide backbone consisting of mannose and arabinose that are further elaborated by either mannooligosaccharide or phosphoinositol caps, representing the third domain, and resulting in LAM being termed ManLAM (14, 15) or PILAM (16, 17), respectively. In addition, a new class of LAM, isolated and characterized from *Mycobacterium chelonae*, has been shown to be devoid of any capping motifs, and is termed AraLAM (18).

Both ManLAM and PILAM exhibit a broad range of immunomodulatory activities. For example, ManLAM inhibits a number of the immune system effector functions, including interferon-γ-mediated activation of macrophages (19–21). Moreover, ManLAM can inhibit the production of pro-inflammatory cytokines, interleukin-12 (22) and tumor necrosis factor-α (23). Thus, it appears that slow growing mycobacteria possess a virulence factor enabling their persistence within the host. Conversely, PILAM can induce a pro-inflammatory re-

* This work was supported in part by Medical Research Council Grants G9901077 and G9901078 and by Wellcome Trust Grant 058972. The costs of publication of this article were defrayed in part by the payment of page charges. This article must therefore be hereby marked "*advertisement*" in accordance with 18 U.S.C. Section 1734 solely to indicate this fact.

‖ Jenner Research Fellow of the Lister Institute. To whom correspondence should be addressed. Tel.: 44-121-415-8125; Fax: 44-121-414-5925; E-mail: g.besra@bham.ac.uk.

[1] The abbreviations used are: PIM, phosphatidyl-*myo*-inositol mannoside; LB, Luria-Bertani; LAM, lipoarabinomannan; LM, lipomannan; MALDI-MS, matrix-assisted laser desorption/ionization-mass spectrometry; ManLAM, lipoarabinomannan with mannose caps; Man*p*, mannopyranose; MPI, mannosyl-phosphatidyl-*myo*-inositol anchor; PBS, phosphate-buffered saline; PI, phosphatidyl-*myo*-inositol; PILAM, lipoarabinomannan with phosphoinositide caps; PPM, polyprenol monophosphomannose; TLC, thin layer chromatography; t, terminal.

[2] PIM nomenclature is taken from Kordulakova *et al*. (1). PIM is used to describe the global family of phosphatidyl-*myo*-inositol mannosides that carry one to four fatty acids (attached to the glycerol, *myo*-inositol, and/or mannose and one to six mannose residues. In Ac_xPIM_y, *x* refers to the number of acyl groups esterified to the *myo*-inositol or mannose residues, and *y* refers to the number of mannose residues. For example, Ac_1PIM_2 corresponds to the phosphatidyl-*myo*-inositol dimannoside, carrying two acyl groups attached to the glycerol (the diacylglycerol moiety) and one acyl group esterified to the mannose or inositol residue.

sponse in a Toll-like 2 receptor (TLR-2) dependent manner (24), and as a consequence PILAM are likely to favor the killing of fast growing mycobacteria. The biological importance of the capping motifs found in ManLAM is now without doubt, reinforcing an emerging paradigm that "capped" LAM molecules possess immunomodulatory type properties (22, 25, 26).

A number of non-mycobacterial actinomycetes possess lipoglycans, including *Rhodococcus ruber* (27), *Rhodococcus equi* (28), *Amycolatopsis sulfurea* (29), and *Tsukamurella paurometabola*.[3] Structurally, these lipoglycans are related to mycobacterial LAM, but are typically smaller in size. Nevertheless, they possess a similar global architecture, with the most significant difference related to the degree of arabinosylation and mannosylation. Thus, it would seem that these close relatives have evolved a specific set(s) of enzymes dedicated to the production of these biosynthetically related PIMs, LM and LAM. As a result, a plethora of information exists to study lipoglycan biosynthesis within the Actinomycetales family, through the use of genomic and metabolomic approaches, linked to the use of more genetically tractable species, such as the industrial important bacilli, *C. glutamicum*.

Although the structure of mycobacterial LAM has been well documented (10–13), the genetics of its biosynthesis still remain largely ill defined. It involves the addition of Man*p* residues to phosphatidyl-*myo*-inositol (PI) to produce both the short PIMs (2–6 Man*p* residues) and LM, which is further glycosylated with arabinan to form LAM. The biosynthetic relationship of PI → PIMs → LM → LAM has recently been supported by biochemical (30, 31) and genetic studies (32–34). Besra *et al.* (31) demonstrated that Ac_1PIM_2 (according to the nomenclature of Kordulakova *et al.* (Ref. 1)) is specifically extended by the addition of Man*p* residues from the alkali-stable sugar donor polyprenyl monophosphomannose (PPM) to form higher PIMs and "linear" LM. The generation of PPM, which results from the transfer of Man*p* from GDP-Man*p* to a polyprenyl phosphate, has been studied in *M. tuberculosis* H37Rv, and is catalyzed by a PPM synthase, now termed *Mt-ppm1* (*Rv2051c*) (35).

In the present study we have established that *C. glutamicum* possess both PIMs and lipoglycans, which are reminiscent of *M. tuberculosis* products, suggesting conserved biosynthetic machineries within the two bacilli. Furthermore, through comparative genomic analyses, we have identified the corynebacterial PPM synthase *Cg-ppm1*, analogous to *Mt-ppm1/D2*. The disruption of *Cg-ppm1* through homologous recombination led to a lipoglycan-less phenotype. In addition, complementation with *Mt-ppm1/D2* led to restoration of lipoglycan biosynthesis in *C. glutamicum*. These results demonstrate the first biochemical and molecular description of lipoglycan biosynthesis in a non-mycobacterial species and highlight the inherent usefulness of examining related species to probe complex biosynthetic pathways.

EXPERIMENTAL PROCEDURES

Bacterial Strains and Growth Conditions—*Escherichia coli* DH5αmcr and *C. glutamicum* ATCC 13032 (the wild type strain, and referred to for the remainder of the text as *C. glutamicum*) were grown in Luria-Bertani (LB) broth (Difco) at 37 and 30 °C, respectively. The mutants generated by this study were grown on complex medium LB-HIS (which contained per liter: 5 g of tryptone, 5 g of NaCl, 2.5 g of yeast extract, 18.5 g of brain heart infusion (Difco Labs Ltd, Surrey, UK), and 90.1 g of sorbitol). Antibiotics were used at the following concentrations: 50 μg/ml kanamycin, 10 μg/ml chloramphenicol, and 10 μg/ml tetracycline. Growth curves were performed using the minimal medium CGXII (36), except that 30 mg/liter protocatechuic acid was included as a chelating agent. Mutants were grown overnight on LBHIS, harvested, washed once with 0.9% NaCl, and inoculated into CGXII to give a starting optical density of 1, harvested again, washed once with 0.9% NaCl, and lyophilized. For lipid and lipoglycan analyses, along with crude cellular extract preparations, cells were grown in an identical manner. For the preparation of membranes, bacterial strains were grown in LB broth, supplemented with antibiotics, grown to mid log phase, harvested by centrifugation, washed with PBS (50 mM, pH 7.5), and stored at −20 °C until further use.

Plasmids and DNA Manipulation—To enable inactivation of *Cg-ppm1* in the chromosome of *C. glutamicum*, the plasmid pK18mob-Cg-ppm1-int was generated. An internal fragment of *Cg-ppm1* was amplified via PCR using primers 5′-CCCTGCGGTCATATCGGTCA-3′ and 5′-GCGTACATGGCTGGCTTCCA-3′. The resulting fragment was purified via gel electrophoresis and ligated with *Sma*I-cleaved pK18mob (37), using the SureClone ligation kit (Amersham Biosciences, Uppsala, Sweden).

Overexpression of *Mt-ppm1/D2* was obtained with pXMJ19-Mt-ppm1/D2. The primers used were 5′-GC**TCTAGA**AAGGAGATATAGATATGACCACCGGCCAGCC-3′ and 5′-C**GGAATT**CTTATTCGGTCACGTCGGCGC-3′ (with the cloning sites in bold and the ribosome binding site and start codon, introduced to enable expression of domain D2 of *Mt-ppm1*, underlined). The amplified fragment was purified, treated with *Xba*I and *Eco*RI, and ligated with similarly treated pXMJ19 (38) to give pXMJ19-Mt-ppm1/D2.

Overexpression of *Cg-ppm1* was obtained with pVWEx2-Cg-ppm1. The primers used were 5′-GCTCTAGAAAGGAGATATAGATATGAGCAGTGAGGCAGTAGAT-3′ and 5′-CGGGATCCTTAGAGCCAGGTGTTGCGC-3′. The fragment was cloned with the SureClone ligation kit in pUC18, excised as an *Xba*I/*Bam*HI fragment from the resulting vector, and ligated with similarly treated pVWEx2.

The in-frame deletion of *Cg-ppm2* in *C. glutamicum* was achieved with pK19mobsacB-Cg-ppm2. This plasmid was made using cross-over PCR (39) to enable the one-ligation step integration of upstream together with downstream sequences of *Cg-ppm2* into pK19mobsacB (37). Using the Expand Highfidelity PCR system (Roche, Basel, Switzerland) in the first PCR round, two separate amplification products were generated with 5′-CGCGGATCCGAGCGCGACGCTGATGTAGAC-3′ (*Cg-ppm2*-3′-out)/5′-ACAAATTCAAATCACCTACCCGCGAAAAAGGCAGCAACTAATCG-3′ (*Cg-ppm2*-3′-in) and with 5′-CGCGATCCGCGGGCCAAGCGCATGCGCAGTG-3′ (*Cg-ppm2*-5′-out)/5′-GGGTAGGTGATTTGAATTTGTAGTTGGGCCCGTGGACATCT-3′ (*Cg-ppm2*-5′-in). Both PCR products were purified and used as a template to amplify, with primers *Cg-ppm2*-5′-out and *Cg-ppm2*-3′-out, a fragment devoid of *Cg-ppm2* that was treated with *Bam*HI and ligated with *Bam*HI-cleaved pK19mobsacB to give pK19mobsacB-Cg-ppm2. The inserts in all final constructs were confirmed by sequencing.

Construction of Strains—Plasmids were usually introduced via electroporation, but conjugation was used when electroporation failed. Conjugation was done with *E. coli* S-17-1 as the donor, and its sensitivity to nalidixic acid (50 μg/ml) was used after plating for counterselecting. Selection of recombinant *C. glutamicum* strains for the presence of the replicative plasmid pVWEx2-Cg-ppm1 used 2 μg/ml tetracycline, and pXMJ19-Mt-ppm1/D2 used 5 μg/ml chloramphenicol. The *ppm1* gene was inactivated in *C. glutamicum* by transformation with pK18mob-Cg-ppm1-int. A recombinant strain was selected with 15 μg/ml kanamycin and the chromosomal inactivation confirmed by PCR. The resulting strain was termed *C. glutamicum*::ppm1.

To achieve deletion of *Cg-ppm2*, plasmid pK19mobsacB-Cg-ppm2 was introduced into *C. glutamicum* by conjugation. Selection for resistance to kanamycin yielded two clones, indicating integration of the vector in the chromosome by homologous recombination. Each of the clones was subjected to the subsequent selection for the second homologous recombination event. In this round the presence of *sacB* (together with addition of 10% sucrose to the medium) resulted in a positive selection of clones where vector sequences were lost again (37). The correct integration of sequences into the chromosome and absence of sequences, respectively, in the resulting strain, *C. glutamicum*Δppm2, was verified by PCR using two different primer pairs.

Extraction of Whole Cell Lipids—Lyophilized *C. glutamicum*, *C. glutamicum*::ppm1, and *C. glutamicum*::ppm1 pMt-ppm1/D2 were extracted by three consecutive overnight extractions in $CHCl_3/CH_3OH$ (2:1, v/v). These lipidic extracts were combined, dried under reduced pressure, Folch-washed, $CHCl_3/CH_3OH/H_2O$ (4:2:1, v/v/v), and again dried under reduced pressure and analyzed by MALDI-MS.

Extraction of Lipoglycans—500 mg of lyophilized cells of *C. glutamicum*, *C. glutamicum*::ppm1, and *C. glutamicum*::ppm1 pMt-ppm1/D2 were delipidated as described above. The delipidated cells were then resuspended in 10 ml of PBS (50 mM, pH 7.5) and 10 ml of phenol-

[3] K. J. C. Gibson and G. S. Besra, unpublished results.

saturated PBS and incubated with stirring at 90 °C for 60 min (40, 41). The mixture was then centrifuged at 4500 × *g* for 10 min and the upper aqueous phase removed and dialyzed for 24 h against water, with frequent changes. The recovered samples, containing lipoglycans and glycans, were dried under reduced pressure and resuspended in 500 μl of 15% propan-1-ol in 50 mM ammonium acetate buffer and loaded onto an octyl-Sepharose CL-4B column (Sigma UK, 30 × 1.5 cm) and eluted with 3 column volumes of the same buffer at 5 ml/h, enabling the removal of non-lipidic moieties (22). The retained lipoglycans were eluted with 3 column volumes of 50% propan-1-ol in 50 mM ammonium acetate buffer. The resulting lipoglycans were either analyzed by SDS-PAGE, followed by periodic acid-silver nitrate staining, or subjected to further purification using gel filtration chromatography, as described by Gibson *et al.* (29), for glycosidic linkage analysis.

Glycosidic Linkage Analysis—Glycosyl linkage composition was performed according to the modified procedure from Ciucanu and Kerek (42). The per-*O*-methylated lipoglycans were hydrolyzed using 500 μl of 2 M trifluoroacetic acid at 110 °C for 2 h, reduced using 350 μl of a 10 mg/ml solution of $NaBD_4$ (1 M ammonium hydroxide/ethanol; 1:1, v/v) and per-*O*-acetylated using 300 μl of acetic anhydride for 1 h at 110 °C. The resulting alditol acetates were solubilized in cyclohexane before analysis by gas chromatography and gas chromatography coupled to mass spectrometry.

Preparation of Enzyme Fractions—*C. glutamicum*, *C. glutamicum*::ppm1, and *C. glutamicum*::ppm1 pMt-ppm1/D2 were grown (10 g wet weight), washed, and re-suspended in 30 ml of buffer A, which contained 50 mM MOPS (adjusted to pH 8.0 with KOH), 5 mM β-mercaptoethanol, and 10 mM $MgCl_2$, at 4 °C and subjected to sonication (Soniprep 150, MSE Sanyo Gallenkamp, Crawley, Sussex, UK; 1-cm probe) for a total of 10 cycles in 60-s pulses and 90-s cooling intervals. The sonicates were centrifuged at 27,000 × g for 60 min at 4 °C. Membrane fractions from the three strains were obtained by further centrifugation of the supernatant at 100,000 × *g* for 90 min at 4 °C. The supernatant was carefully removed and the membranes gently resuspended in buffer A. Protein concentrations were determined using the BCA Protein Assay Reagent kit (Pierce Europe, Oud-Beijerland, Netherlands).

Mannosyltransferase Assays—Membrane fractions from *C. glutamicum* were assayed and compared with *C. glutamicum*::ppm1 and *C. glutamicum*::ppm1 pMt-ppm1/D2 for *in vitro* mannosyltransferase activity, using methods adapted from Besra *et al.* (31). Reaction mixtures contained 95 μg of membranes (total protein), buffer A, 0.1 mM dithiothreitol, and 10 mM $CaCl_2$ either with or without 5 μg of amphomycin (a lipopeptide antibiotic that specifically inhibits polyprenyl-P-requiring synthases and the subsequent synthesis of polyprenol-P-Man) in a total volume of 50 μl. Reactions were incubated for 10 min at 37 °C prior to the addition of 0.25 μCi of GDP-[^{14}C]Man (Amersham Biosciences; 303 mCi/mmol) and held at 37 °C for an additional 30 min. The reactions were stopped by the addition of 4 ml of $CHCl_3/CH_3OH/H_2O$ (10:10:3, v/v/v) and incubated at room temperature for 30 min, followed by the addition of 1.75 ml of $CHCl_3$ and 0.75 ml of H_2O. The lower organic layer of the biphasic mixture was washed three times with 2 ml of $CHCl_3/CH_3OH/H_2O$ (3:47:48, v/v/v), dried under a stream of nitrogen, and resuspended in 200 μl of $CHCl_3/CH_2OH$ (2:1, v/v). The transfer of [^{14}C]Man from GDP-[^{14}C]Man to the *in vitro* synthesized PI/PIMs was quantified by scintillation counting using 5 ml of Ecolume™ (ICN Biomedicals, Costa Mesa, CA) and the materials analyzed by thin layer chromatography (TLC)/autoradiography as described previously (34).

Analysis of Reaction Products—Large scale reaction mixtures containing unlabeled GDP-Man (80 mM) and the other components were prepared and processed as described above. The reaction products were dried, applied to preparative TLC plates (plastic-backed plates of Silica gel 60 F_{254}; E. Merck, Darmstadt, Germany) along with radiolabeled material (50,000 cpm) to trace the cold enzymatically synthesized products and developed in $CHCl_3/CH_3OH/NH_4OH/H_2O$ (65:25:0.5:3.6, v/v/v/v). Autoradiography was performed as described previously (34). The band corresponding to the new enzymatically synthesized PIM product was recovered from plates using 4 ml of $CHCl_3/CH_3OH/H_2O$ (10:10:3, v/v/v) at room temperature for 30 min followed by the addition of 1.75 ml of $CHCl_3$ and 0.75 ml of H_2O. The lower organic layer of the biphasic mixture was washed three times with 2 ml of $CHCl_3/CH_3OH/H_2O$ (3:47:48, v/v/v), dried under a stream of nitrogen, and analyzed using MALDI-MS, as described previously (33).

Polyprenol Monophosphomannose Synthase Assays—Reaction mixtures assessing [^{14}C]Man incorporation consisted of 0.25 μCi of GDP-[^{14}C]Man (Amersham Biosciences; 303 mCi/mmol), 62.5 μM ATP, 10 μM $MgCl_2$, and 90 μg of membrane preparations, prepared as described previously, in a final volume of 50 μl (35). In some cases, exogenous lipid monophosphate substrates (C_{35}, heptaprenyl monophosphate; C_{40}, octaprenyl monophosphate; C_{50}, decaprenyl monophosphate; C_{55}, undecaprenyl monophosphate; and C_{60}, dodecaprenyl monophosphate) were added to reaction mixtures at a final concentration of 0.25 mM in 0.25% CHAPS. The reaction mixtures were then incubated at 37 °C for 30 min.

Extraction and Characterization of [^{14}C]Mannose-labeled Products from PPM Reaction—The above enzymatic reactions were terminated by the addition of 4 ml of $CHCl_3/CH_3OH$/0.8 M NaOH (10:10:3, v/v/v) followed by further incubation at 50 °C for 20 min. The mixtures were then allowed to cool to room temperature, and 1.75 ml of $CHCl_3$ and 0.75 ml of H_2O were added. The mixture was vortexed and centrifuged, and the upper aqueous phase discarded. The organic phase was washed three times with 2 ml of $CHCl_3/CH_3OH/H_2O$ (3:47:48, v/v/v), dried under a stream of nitrogen to yield an organic fraction, which contained exclusively the mild-alkali stable family of PPMs. The resulting PPMs were resuspended in 200 μl of $CHCl_3/CH_3OH$ (2:1, v/v), and aliquots (20 μl) were dried under a stream of nitrogen in a scintillation vial prior to scintillation counting using 5 ml of Ecolume™ (ICN Biomedicals). Thin layer chromatography of the reaction mixtures, usually aliquots representing 10% of the reaction mixtures, was conducted on aluminum-backed plates of Silica gel 60 F_{254} (E. Merck, Darmstadt, Germany) using $CHCl_3/CH_3OH/NH_4OH/H_2O$ (65:25:0.4:3.6, v/v/v/v). Autoradiograms were obtained as described previously (34).

RESULTS

Genome Comparison of the ppm Locus—Previous work has identified that there are subtle variations in the organization of the *ppm1* locus in mycobacterial strains (35). The well characterized *Mt-ppm1* gene of *M. tuberculosis* is a large polypeptide consisting of two domains, *Mt-ppm1/D1* (functional domain) and *Mt-ppm1/D2* (catalytic domain), shown in Fig. 1*A*. However, a great deal of heterogeneity pertaining to this gene is evident within several mycobacterial species. For instance, in *Mycobacterium smegmatis* these domains are encoded by two separate genes, encoding *Ms-ppm1* and *Ms-ppm2* (Fig. 1*A*), which have recently been shown to interact with each other *in vivo* as revealed by a bacterial two-hybrid system (43).

To gain information on the presence and organization of orthologous genes in related bacteria like *C. glutamicum*, and to analyze for the existence of paralogues, the *Mt-ppm1/D1* and *Mt-ppm1/D2* domains were blasted individually against the genomes of selected Corynebacterianeae in the hope of understanding the genetic organization of these genes within other members of this family. A phylogenetic tree constructed for the closest homologues of *Mt-ppm1/D1* is shown in Fig. 1*B*. Interestingly, a very similar tree was obtained for the polypeptides that are orthologous to *Mt-ppm1/D2*, suggesting their common evolution together with D1 polypeptides (Fig. 1*C*). Indeed, with further comparison of the 16 S ribosomal RNA tree (Fig. 1*D*), there is evidence that both D1 and D2 polypeptides were already present before species separation occurred within the Corynebacterianeae, and that they were retained during vertical descent. When this evidence is taken together, one may conclude that these polypeptides catalyze core functions within this suborder of the Actinomycetales. In addition, the presence of an additional D2 paralogue in *C. glutamicum* (Fig. 1*C*) is apparently a more recent evolutionary event, because a phage integrase site is directly adjacent to the corresponding gene; moreover, this is absent in the closest related species, *Corynebacterium efficiens* (Fig. 1*D*).

Through further analysis of the *M. tuberculosis* and *M. avium* genomes, we identified the presence of two sequences that are distantly related to *Mt-ppm1/D2* (not shown in Fig. 1*C*). Interestingly, a gene that is of similar size to *Mt-ppm1/D1* directly precedes these sequences; furthermore, these preceding genes also encode a protein with transmembrane domains. One may assume that, with this level of genetic organization, these paralogues are organized within an operon, and might constitute a functional complex similar to *Mt-ppm1*. Indeed, it would appear that both D1 and D2 domains are general struc-

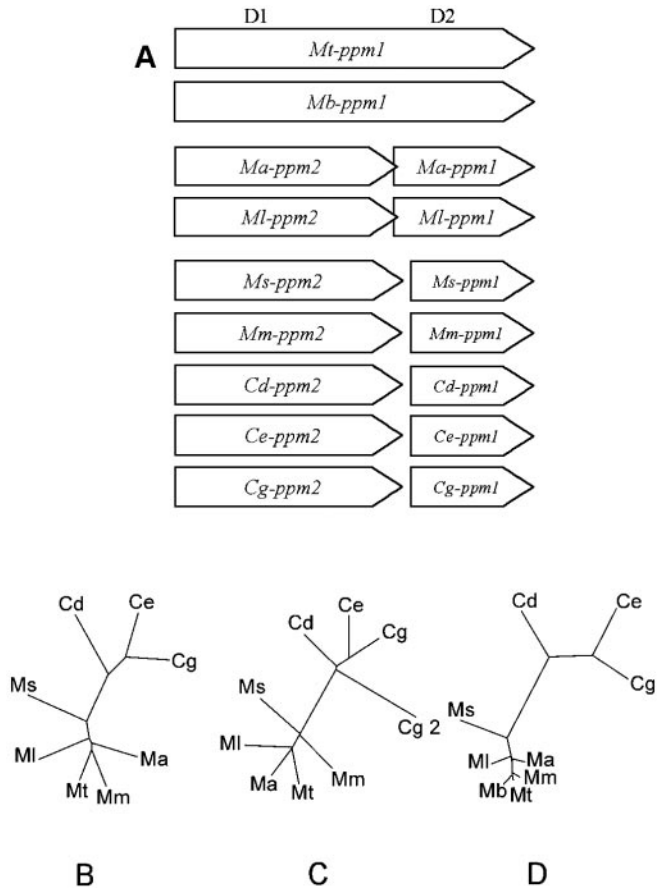

FIG. 1. **The *ppm* locus in the Corynebacterianeae and the relatedness of the separate encoded domains**. *A*, an overview of the genetic organization is shown with both genes either fused (*top*), overlapping (*middle*), or separated (*bottom*). A fusion is present in *M. tuberculosis* H37Rv (*Mt-ppm1*) and further members of this complex including *M. bovis* (*Mb-ppm1*). The genes are overlapping in the case of *M. avium* (*Ma-ppm2*, *Ma-ppm1*) and *M. leprae* (*Ml-ppm2*, *Ml-ppm1*). The genes are separated in the case of *M. smegmatis* (*Ms-ppm2*, *Ms-ppm1*), *M. marinum* (*Mm-ppm2, Mm-ppm1*), *C. diphtheriae* (*Cd-ppm2*, *Cd-ppm1*), *C. efficiens* (*Ce-ppm2*, *Ce-ppm1*), and *C. glutamicum* (*Cg-ppm2*, *Cg-ppm1*). *B*, an unrooted phylogenetic tree of the D1 domains is shown, and in *C* a similar tree for the D2 domains. *D*, the phylogenetic tree is shown comparing the Corynebacterianeae under study, as derived from the 16 S ribosomal RNA sequences.

tural elements that occur more frequently in mycobacteria than in corynebacteria.

In all Corynebacterial species examined to date, both *ppm* domains are encoded by non-overlapping genes, which is also the case in *M. smegmatis* and *Mycobacterium marinum*, with the largest gap of 32 bp present in *C. glutamicum*. In contrast, members of the *M. tuberculosis* complex (H37Rv, CDC1551, *Mycobacterium bovis*) exhibit a different level of genetic organization, whereby both domains are fused to generate one multifunctional polypeptide (Fig. 1*A*). This difference may indicate a more recent episode of protein evolution, which is in accord with the notion that this branch of slow growing mycobacteria represents the most recently evolved subset of the genus (44).

Construction of C. glutamicum ppm Mutants—The gene domains identified as orthologous to *Mt-ppm1* in *C. glutamicum* were preliminarily termed *Cg-ppm1* and *Cg-ppm2*, catalytic domain and putative transmembrane domain, respectively, according to the known function of *ppm1* in *M. tuberculosis* (35) and consistent with the sequence and conserved genome structure of both organisms.

To inactivate *Cg-ppm1*, the non-replicative plasmid pK18-mob-Cg-ppm1-int was used to transform the *C. glutamicum* wild type to kanamycin resistance (Fig. 2*A*). Six colonies were obtained, all exhibiting smaller colony sizes than the wild type, approximately 0.5 and 2 mm, respectively, when grown at 30 °C for 2 days on LB media. One of the recombinant clones was analyzed in detail via PCR. For this purpose two different primer pairs were used, each pair hybridizing with vector and *Cg-ppm1* sequences. In both cases the expected fragment was obtained, confirming the integration of the vector into the target gene (Fig. 2, *A* and *C*). The disruption mutant obtained was termed *C. glutamicum*::ppm1. In addition, a strain with an in-frame deletion of *Cg-ppm2*, termed *C. glutamicum*Δppm2, was generated (shown in Fig. 2, *B* and *C*), and included in growth studies.

Growth of C. glutamicum Mutants—To assay for any potential *in vivo* function of *Cg*-Ppm1 and *Cg*-Ppm2, growth rates of the generated mutants and controls were analyzed in liquid culture using salt medium. As seen in Fig. 3, the growth rate of *C. glutamicum*::ppm1 was impaired. Indeed, the growth rate of the mutant was 0.25 h^{-1} as compared with 0.34 h^{-1}, obtained for the wild type. The optical density of *C. glutamicum*::ppm1 only became comparable with that of the wild type after 25 h of growth. As expected, when pVWEx2-Cg-ppm1 was introduced into *C. glutamicum*::ppm1, with the resulting strain referred to as *C. glutamicum*::ppm1 pCg-ppm1, growth was restored to a rate equivalent to wild type (Fig. 3). This result indicates that *Cg-ppm1* is not an essential gene for growth, although it is required for optimal growth rate. Electron microscopic analyses of the mutated cells did not reveal any ultrastructural changes when compared with the wild type (data not shown). Intriguingly, when the growth rate of the strain *C. glutamicum*Δppm2 was assayed, which does not possess the protein domain corresponding to *Mt*-Ppm1/D1, no effect on growth rate was observed (Fig. 3). This has been assigned as a putative transmembrane domain that is thought to play a role in stabilizing the catalytic domain (*Cg*-Ppm1, or *Mt*-Ppm1/D2) (35, 43). With this result one can draw two conclusions: that the exact *in vivo* roles of *Cg*-Ppm2, or *Mt*-Ppm1/D1 are not completely understood, or that, if required, *Cg*-Ppm1 or *Mt*-Ppm1/D2 may be able to self-stabilize in close proximity to the membrane, as suggested previously.

In *C. glutamicum* a paralogue of *Cg-ppm1* is present, which is of similar length (250 instead of 270 amino acids) and shares 76% identity with the gene product of *Cg-ppm1*. Nevertheless, when the plasmid-encoded paralogue was introduced to *C. glutamicum*::ppm1, no restoration of growth rate was observed (data not shown), which might indicate, together with the apparent recent origin, that this gene is a non-functional copy.

Expression of Mt-ppm1/D2 and Functional Complementation of C. glutamicum::ppm1—Plasmid pXMJ19-Mt-ppm1/D2 was constructed to contain domain 2 of the *M. tuberculosis ppm1* gene, extending from amino acid residue 594 to residue 874. In the plasmid a start codon and an appropriate ribosome-binding site were introduced. In this study the plasmid was used to transform *C. glutamicum*::ppm1 to give *C. glutamicum*::ppm1 pXMJ19Mt-ppm1/D2, with the resulting strain referred to as *C. glutamicum*::ppm1 pMt-ppm1/D2. When a crude cellular extract of this complemented strain was analyzed by SDS-PAGE, an extra protein band was observed that was absent in the uncomplemented mutated strain (Fig. 4, *lanes 3* and *2*, respectively). MALDI-MS analyses identified tryptic digests of the *Mt*-Ppm1/D2 fragments with a coverage >40% (data not shown). Therefore, domain 2 of the mycobacterial polyprenyl monophosphomannose synthase is able to form a stable protein in *C. glutamicum*::ppm1, an expected result that confirms the

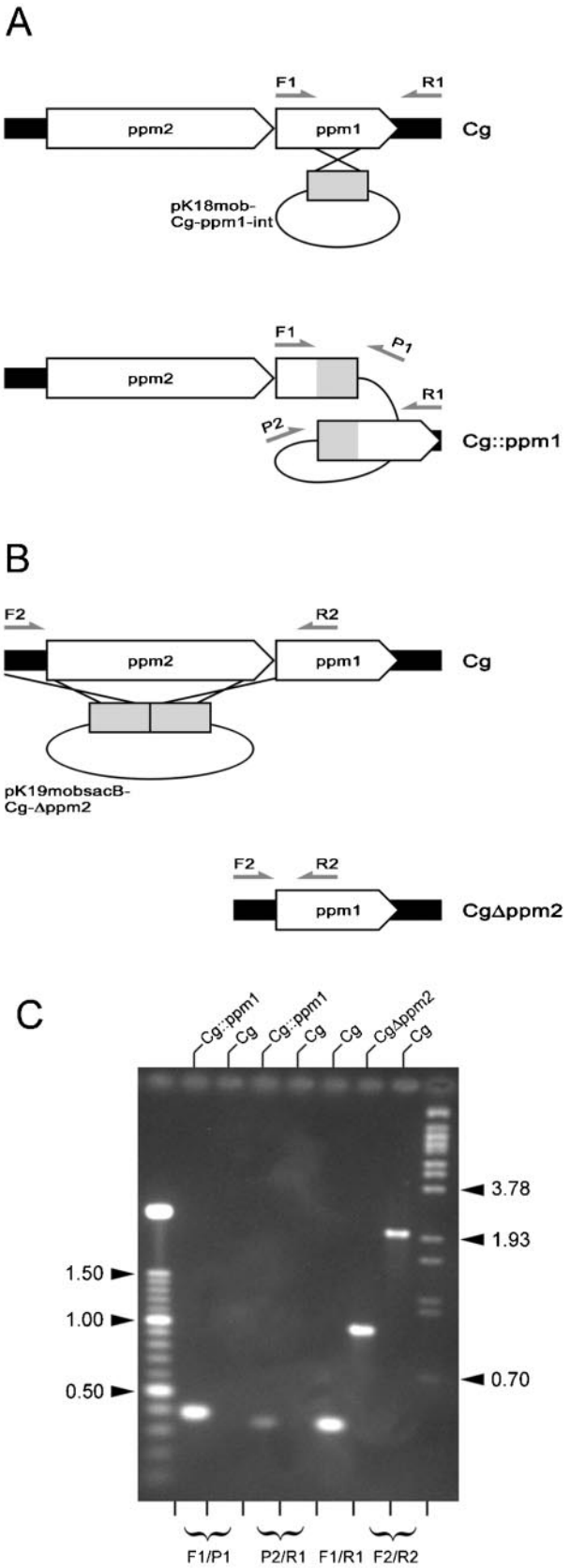

FIG. 2. **Schematic diagram for the construction of the *ppm* mutants derived from *C. glutamicum*.** *A*, illustrated are the adjacent *ppm1* and *ppm2* genes and the strategy to disrupt *ppm1* using the inactivation vector pK18mob-Cg-*ppm1*-int. The inactivation vector carries an internal 247-bp fragment of *ppm1*, given as a *shaded box*. Homologous recombination and selection for kanamycin resistance results in strain *Cg*::ppm1 with disrupted *ppm1* and without Ppm1 activity. The location of the three different primer pairs to confirm the chromosomal organization of *ppm1* are indicated as *arrows* marked *F1/R1*, *F1/P1*, and *P2/R1*. *B*, strategy to delete the entire structural gene of *ppm2* using vector pK19mobsacB-Cg-Δppm2. This vector carries sequences of 563 and 467 bp, respectively, which are identical to sequences directly flanking *ppm2* and which are fused in pK19mobsacB-Cg-Δppm2. This vector carries the kanamycin resistance gene, as well as *sacB* enabling two rounds of positive selection for integration of the vector, and subsequent loss of the vector, respectively. The location of the two primers used to confirm the chromosomal organization of *ppm2* are indicated as *arrows* marked *F2/R2*. *C*, final confirmation of the constructed strains via PCR analysis using chromosomal DNA from *C. glutamicum*, of the *ppm1* inactivation mutant (*Cg*::ppm1), and of the *ppm2* deletion mutant (*Cg*Δppm2). The *outer lanes* contain standards with their sizes given in kb. With the primer pairs given as indicated, the expected product sizes for analysis of the *ppm1* locus were 377 and 350 bp, respectively, for strain *Cg*::ppm1 and 349 bp for *C. glutamicum*. For analysis of the *ppm2* locus, the expected product sizes were 1051 bp for strain *Cg*Δppm2 and 2419 bp for *C. glutamicum*.

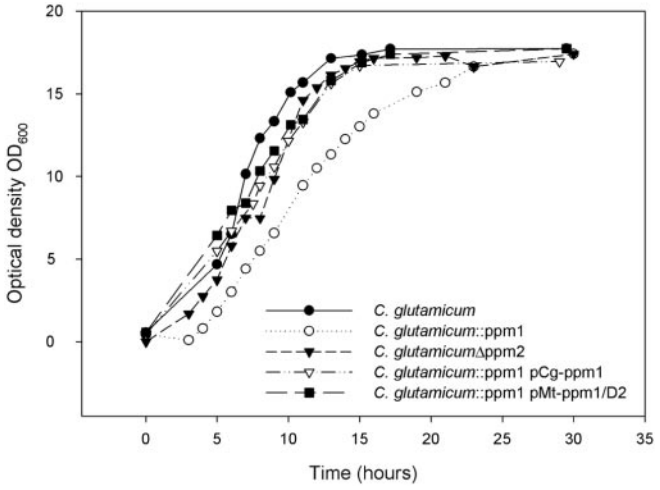

FIG. 3. **Growth curve illustrating the effects on growth rate after inactivation of *Cg-ppm1* or deletion of *Cg-ppm2*.** The effect of inactivating *Cg-ppm1* (*C. glutamicum*::ppm1) or deletion of *Cg-ppm2* (*C. glutamicum*Δppm2), as compared with wild type *C. glutamicum*, is shown over a 30-h period and measured at an optical density of 600 nm spectrometrically. The effect of inactivating *Cg-ppm1* (*C. glutamicum*::ppm1) and complementation with either a plasmid encoded *Cg-ppm1* (*C. glutamicum*::ppm1 pCg-ppm1) or a plasmid encoded *Mt-ppm1/D2* (*C. glutamicum*::ppm1 pMt-ppm1/D2), as compared with wild type *C. glutamicum*, is also shown.

clear domain and genetic organization of the homologous proteins (Fig. 1*A*).

The growth of the complemented strain (*C. glutamicum*::ppm1 pMt-ppm1/D2) was analyzed as above in salt medium. When the inactivated mutant was complemented with the plasmid containing *Mt-ppm1/D2*, recovery of growth was observed, illustrated in Fig. 3. In summary, *Mt-Ppm1/D2* is able to replace the activity of the corresponding *Cg-ppm1*, and the identified polyprenyl monophosphomannose synthase activities (35) are in part the result of this protein. This confirmed that the *Mt-Ppm1/D2* domain itself is functional, and sufficient to restore growth rate.

Incorporation of GDP-[^{14}C]Mannose by Enzymatic Extracts from C. glutamicum, C. glutamicum::ppm1, and C. glutamicum::ppm1 pMt-ppm1/D2—To further prove that the altered growth rates observed for *C. glutamicum*::ppm1 were the result of this strain lacking a functional copy of a PPM synthase, we examined membrane extracts prepared from *C. glutamicum*, *C. glutamicum*::ppm1, and *C. glutamicum*::ppm1 pMt-ppm1/D2, and compared their relative PPM synthase activities.

Examination of the corynebacterial PPM family by TLC/autoradiography indicated that *C. glutamicum* possess one species of PPM (Fig. 5). To identify the species present in

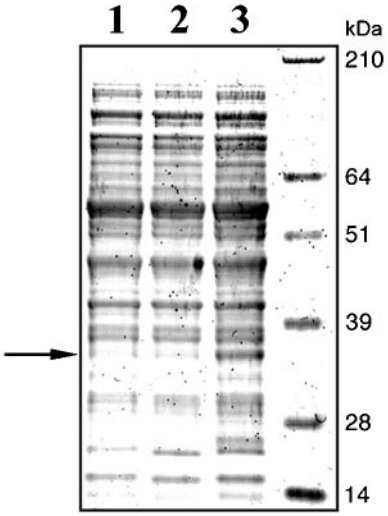

FIG. 4. **SDS-PAGE of crude cellular extracts illustrating overexpression of *Mt-ppm1/D2* in *C. glutamicum*.** Crude cellular extracts were prepared, and in each case 10 μg was subjected to SDS-PAGE (12%) and stained with Coomassie Blue. *Lane 1*, *C. glutamicum*; *lane 2*, *C. glutamicum*::ppm1, empty pXMJ19; *lane 3*, *C. glutamicum*::ppm1 pMt-ppm1/D2. The *arrow* indicates the extra band resulting from the expression of pXMJ19-Mt-ppm1/D2. Molecular masses of reference proteins are indicated.

C. glutamicum, membrane fractions were incubated with and without a range of exogenous commercially available polyprenol monophosphates. With the co-spotting of endogenous and exogenously added PPM molecules, we were unequivocally able to identify the corynebacterial PPM as an undecaprenol phosphate (C_{55}) species (data not shown), similar in chain length to those found in *E. coli* (45). Furthermore, we found, in complete agreement with our previous studies, that the corynebacterial synthase, *Cg*-Ppm1, showed a similar lack of specificity for polyprenyl phosphates in relation to changes in the lipid moiety, such as saturation of the α-isoprenoid unit (35). However, *Cg*-Ppm1 did show a small degree of specificity toward the chain length of exogenous PPM molecules, with the optimal enzymatic activity being observed with chain lengths $> C_{35}$ (data not shown).

As expected the PPM synthase-specific enzymic activity from the wild type strain was clearly evident (12.63 pmol/mg/min), and *C. glutamicum*::ppm1 was found to possess no PPM synthase activity (Fig. 5). The complemented mutant (*C. glutamicum*::ppm1 pMt-ppm1/D2) was assayed for PPM synthase activity, with our results showing a restoration of enzymatic activity to almost 50% of that observed in the wild type strain (5.95 pmol/mg/min) (Fig. 5). The restoration of PPM synthase activity in the complemented mutant, through the use of a plasmid-encoded gene, further emphasizes that domain 2 of the *M. tuberculosis ppm* gene is catalytic, and, as expected, *Cg-ppm1* possesses the PPM synthase activity of the two orthologues identified in the *C. glutamicum* genome. In addition, these results provide further evidence that corynebacteria represent a suitable model enabling functional studies using the expression of mycobacterial genes.

In Vivo and in Vitro Characterization and Analysis of PIM and Lipoglycan Biosynthesis in C. glutamicum—To date, we are not aware of any studies comparing the nature of the *in vivo* and *in vitro* synthesized PIM molecules in corynebacteria. Therefore, we extracted the whole cell lipids, known to contain PIM molecules (46, 47), from *C. glutamicum* and *C. glutamicum*::ppm1 and analyzed these using two-dimensional TLC. As revealed via TLC, both strains produced identical PIM profiles (data not shown). In addition, the *in vivo C. glutamicum* lipids were analyzed by MALDI-MS (Fig. 6). *In vivo*, *C. glutamicum* produces PI ($C_{16}/C_{18:1}$; *m/z* 835) and Ac_1PIM_2 ($2C_{16}/C_{18:1}$; *m/z* 1397) as the major species, as well as a minor component characterized as Ac_1PIM_2 ($C_{16}/C_{18:1}/C_{18}$; *m/z* 1425). Moreover, the identification of these PIM species together with the nature of the acyl groups is in complete agreement with previous work (7).

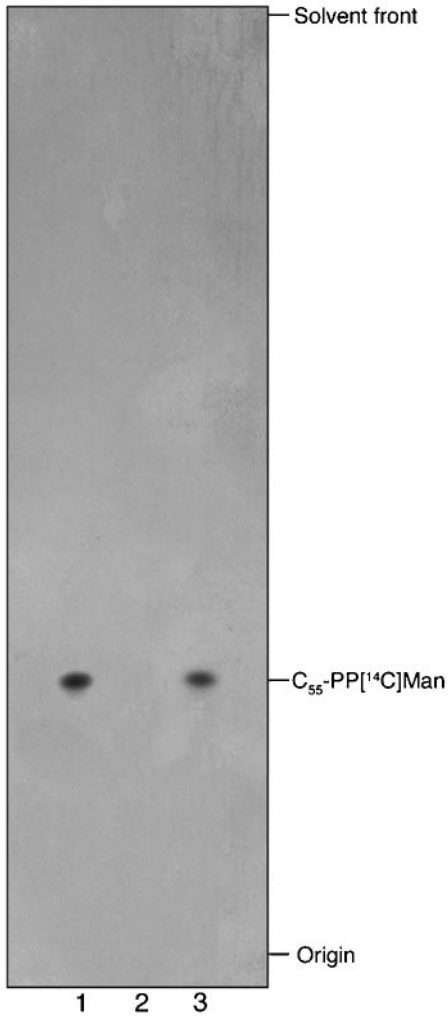

FIG. 5. **Thin layer chromatogram of labeled endogenous polyprenol monophosphates using GDP-[^{14}C]Man and membrane extracts from *C. glutamicum*, *C. glutamicum*::ppm1, and *C. glutamicum*::ppm1 pMt-ppm1/D2.** Membrane fractions were incubated with GDP-[^{14}C]Man in a total volume of 50 μl for 30 min and synthesized products isolated after mild base treatment. Aliquots (10%) were taken for scintillation counting and TLC/autoradiography using $CHCl_3$/CH_3OH/NH_4OH/H_2O (65:25:0.4:3.6, v/v/v/v). *Lane 1*, *C. glutamicum*; *lane 2*, *C. glutamicum*::ppm1; *lane 3*, *C. glutamicum*::ppm1 pMt-ppm1/D2. Assays were performed in triplicate using freshly prepared membranes, with the thin layer chromatogram representative of a number of samples from independent experiments.

With the identification of both lipoglycans and glycolipids in the cell envelope of *C. glutamicum*, we reasoned that both corynebacteria and mycobacteria should possess similar biosynthetic pathways dedicated to the production of these complex polysaccharides. The availability of amphomycin (a lipopeptide antibiotic that specifically inhibits polyprenol-P-requiring synthases, thus blocking the synthesis of C_{55}-P-Man, and the subsequent production of higher PIMs) meant we were able to probe the initial *in vitro* steps involved in the production of PIMs in *C. glutamicum*. Both *C. glutamicum* and *C. glutamicum*::ppm1 were examined for GDP-Man-dependent mannosyltransferase activities associated with PIM biosynthe-

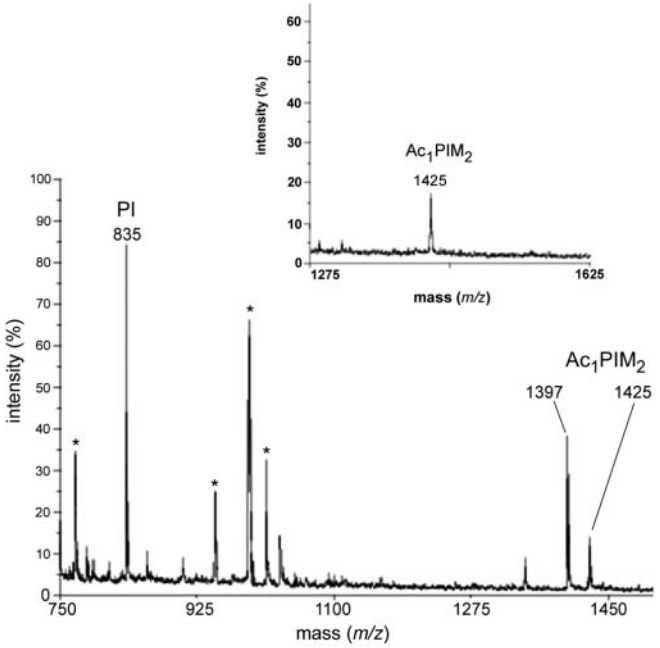

FIG. 6. **Characterization of *in vivo* and *in vitro* synthesized PI/PIMs.** Figure shows negative ion mode MALDI-MS analysis of total lipidic extract from *C. glutamicum*. *Inset*, negative ion mode MALDI-MS analysis of the *in vitro* synthesized PIMs from *C. glutamicum*. The peaks observed are *m/z* 835, PI with $C_{16}/C_{18:1}$ fatty acyl groups; *m/z* 1397, Ac_1PIM_2 with $2C_{16}/C_{18:1}$ fatty acyl groups; and *m/z* 1425, Ac_1PIM_2 with $C_{16}/C_{18:1}/C_{18}$ fatty acyl groups. Major peaks, identified by *asterisks* with *m/z* values of 770, 949, 991, and 1013, respectively, were not attributable to any PIM species and as such may represent unidentified lipid species and/or plasticizer.

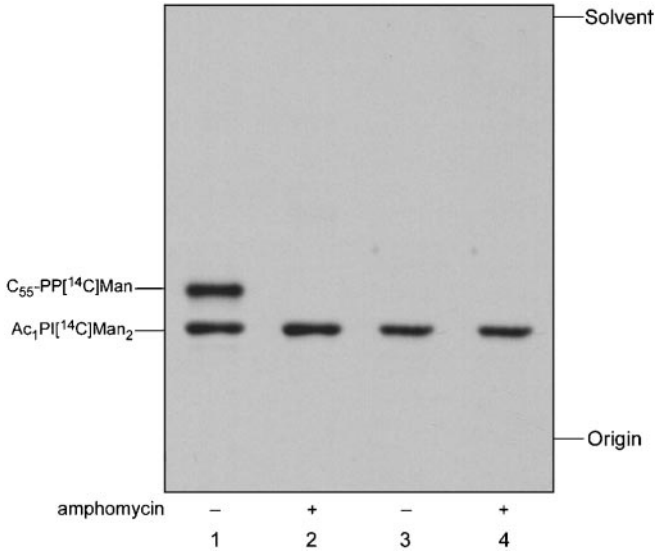

FIG. 7. **Thin layer chromatogram of labeled endogenous PPMs and PIMs using GDP-[^{14}C]Man and membrane extracts from *C. glutamicum* and *C. glutamicum*::ppm1.** Membrane fractions were incubated with GDP-[^{14}C]Man in a total volume of 50 μl for 30 min and synthesized products isolated after aqueous treatment, enabling the recovery of the base-labile PIMs. Aliquots (10%) were taken for scintillation counting and TLC/autoradiography using $CHCl_3/CH_3OH/NH_4OH/H_2O$ (65:25:0.4:3.6, v/v/v/v). *Lane 1*, *in vitro* synthesized PPMs and PIMs from *C. glutamicum*; *lane 2*, *in vitro* synthesized PIMs from *C. glutamicum*, demonstrating the inhibition of PPM synthesis via the addition of amphomycin (5 μg); *lanes 3* and *4*, *in vitro* synthesized PIMs from *C. glutamicum*::ppm1, showing the inability of this mutant to synthesize PPMs with and without the presence of amphomycin, respectively.

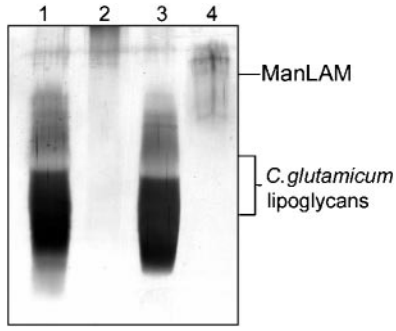

FIG. 8. **SDS-PAGE of lipoglycans extracted from *C. glutamicum*, *C. glutamicum*::ppm1, and *C. glutamicum*::ppm1 pMt-ppm1/D2.** Lipoglycans were extracted from equivalent biomass using the hot phenol/water method and subjected to SDS-PAGE (15%) and stained with periodic acid and silver nitrate. *Lane 1*, sample extracted from *C. glutamicum*; *lane 2*, sample extracted from *C. glutamicum*::ppm1; *lane 3*, sample extracted from *C. glutamicum*::ppm1 pMt-ppm1/D2; *lane 4*, 15 μg of purified *M. tuberculosis* H37Rv ManLAM.

sis using an *in vitro* cell-free assay system. Assays were performed with freshly prepared membranes from both strains. Using thin layer chromatography/autoradiography, we observed one species of *in vitro* synthesized PIM molecules (Fig. 7). Indeed, using large scale assays with unlabeled GDP-Man and *C. glutamicum* membrane preparations, we were able to extract this species and characterize it using MALDI-MS (Fig. 6, *inset*). As expected both strains produced identical products, which were characterized as Ac_1PIM_2 ($C_{16}/C_{18}/C_{18:1}$; *m/z* 1425) (Fig. 6, *inset*). Interestingly, the *in vitro C. glutamicum* membrane extracts synthesize only Ac_1PIM_2 (*m/z* 1425), which is the minor PIM species synthesized by *C. glutamicum in vivo*. The subsequent synthesis of higher PIMs (Ac_1PIM_3, etc.) and linear LM (31) in *C. glutamicum* was completely abrogated because of inhibition of the required C_{55}-P-Man sugar donor by amphomycin, which was also the case, as expected, when we analyzed *C. glutamicum*::ppm1 (data not shown). These results mirror previous studies on the use of amphomycin and the subsequent synthesis of linear LM (31).

Mycobacterial LAM is an important factor in tuberculosis immunopathogenesis, and is a major component in the cell architecture of the tubercle bacilli, along side the other biosynthetically related lipoglycans such as lipomannan and glycolipids including PIMs. These complex lipoglycans are composed of many different carbohydrate residues, with the mannan domain typically composed of 6-Man*p*, 2,6-Man*p*, and *t*-Man*p* residues. The purified lipoglycans from *C. glutamicum* were examined via glycosidic linkage analysis, and the same residues were identified (data not shown). Moreover, through alkaline hydrolysis of the intact lipoglycan, we were able to distinguish C16, C18:1, and C18 fatty acids in the ratio 1:0.6:0.1. Finally, the lipoglycan was hydrolyzed in strong acid conditions and the resulting hydrolysates analyzed using capillary electrophoresis coupled to laser induced florescence. This demonstrated that the lipoglycan was composed exclusively of Man*p* residues (data not shown). Altogether this pointed to the presence of a LM-like lipoglycan within the cell envelope of *C. glutamicum*, and was in complete agreement with the previous work of Puech *et al.* (7). In this study we have previously demonstrated, through the indirect use of amphomycin and the direct use *C. glutamicum*::ppm1, that the formation of higher PIMs and linear LM is dependent on the transfer of mannose from GDP-Man to undecaprenol phosphate, which then acts as the sugar donor for the growing lipoglycan (31, 35). With this in mind, we examined whether *in vivo* lipoglycan biosynthesis was affected by the inactivation of *Cg-ppm1*. Crude lipoglycan extractions were prepared from *C. glutamicum*, *C. glutamicum*::ppm1, and *C. glutamicum*::ppm1 pMt-ppm1/D2. The re-

sults observed were fascinating; the inactivated mutant had lost all ability to synthesize lipoglycans (Fig. 8), which suggests that the amelioration of growth rate observed in the *C. glutamicum*::ppm1 mutant is linked to the production of a full complement of lipoglycans, presumably enabling the bacteria to form a suitable corynebacterial cell envelope. Because we had established that the plasmid-encoded *Mt-ppm/D2* was functional when introduced to *C. glutamicum*::ppm1, we assumed that, when we analyzed the complemented mutant (*C. glutamicum*::ppm1 pMt-ppm1/D2), we would observe restoration of lipoglycan production. Indeed, when the crude lipoglycans were visualized using SDS-PAGE followed by silver nitrate-periodic acid staining, there were no observable differences (Fig. 8), suggesting a key conserved role for this synthase in both mycobacteria and corynebacteria.

DISCUSSION

Mycobacterial LAM is now well accepted as an important immunomodulatory molecule, and plays a significant role in the pathogenesis of tuberculosis. Indeed, a recent study has defined the precise role ManLAM plays in the molecular basis of mycobacterially induced phagosome maturation arrest (48). Moreover, a recent review on mycobacterial LAM suggests that LAM will continue to evolve and emerge as an important virulence factor for tuberculosis (11). Given the importance of this lipoglycan, it appears perplexing that we know very little about the biosynthetic pathways involved in its production and regulation. A number of lipoglycans structurally akin to mycobacterial LAM have been characterized from related Actinomycetales, providing a network of structural information relating to conserved domains within these macromolecules. It seems that the MPI anchor and mannan domain is structurally conserved between genera, whereas the greatest variation is found within the arabinan domain of these LAM-like molecules (11). With the general degree of conservation in both the MPI anchor and mannan region, we chose to undertake a biochemical and molecular study aimed at identifying key enzymes common to both mycobacterial and corynebacterial lipoglycan biosynthesis.

Previous studies have reported the presence of lipoglycans within the corynebacterial cell envelope (7, 9), and our present study has shown that both PIMs and an LM-like molecule exist in *C. glutamicum* and *C. pseudotuberculosis*.[4] These facts support the notion that there are highly conserved biosynthetic pathways within the Actinomycetales family, dedicated to the production of these lipoglycans. The precise *in vivo* role and function of these molecules within the corynebacteria is currently unknown. However, because they are generally nonpathogenic, one may presume they play a crucial role in cell envelope architecture, a fact illustrated by the altered growth rate of the *Cg-ppm1* inactivated mutant described in this study. Further evidence for this hypothesis is provided by the findings of Puech *et al.* (7), who noted that the corynebacterial cell envelope does not contain enough mycolic acids to cover the entire cell surface (7). They suggested that non-covalently associated lipids may compensate for the lack of mycolic acids, and enable the production of a satisfactory hydrophobic cell envelope (7). From our findings it would appear that glycolipids and lipoglycans, also non-covalently associated macromolecules, play a role in determining overall cell architecture, and could supplement the lipids present in the cell envelope.

Detailed genomic analysis of *C. glutamicum* revealed orthologues of *Mt-ppm1* (*Rv2051c*), which were termed *Cg-ppm2* (transmembrane domain, orthologue of *Mt-ppm1/D1*) and *Cg-ppm1* (catalytic domain, orthologue of *Mt-ppm1/D2*). This level of organization is in contrast to that found in *M. tuberculosis* H37Rv, where *Mt-ppm1* has been postulated to be the result of a recent genetic fusion, resulting in a single bi-functional gene, where *Mt-ppm1/D1* is the transmembrane domain and *Mt-ppm1/D2* possesses catalytic activity (35). The genetic arrangement of the corynebacterial orthologues is more reminiscent of the *ppm* genes found in other mycobacterial strains such as *M. avium*, *M. smegmatis*, and *M. leprae*, as shown in Fig.1*A*.

The present study highlights the overall importance of the Ppm synthase in lipoglycan biosynthesis. We have established that, when *C. glutamicum* lacks a functional copy of *Cg-ppm1*, it is unable to produce any mature lipoglycans, but can still produce PIMs. The importance of these findings has wider implications for several reasons. First, a number of reports have identified several mannosyltransferases, termed *pimA*, *pimB*, and *pimC* within mycobacterial genomes, which have been shown to be involved in PIM_{1-3} biosynthesis (32–34). *pimA* has been shown to be essential for mycobacterial growth, as it initiates lipoglycan biosynthesis through the production of PIM_1. In contrast, both *pimB*[5] and *pimC* have been shown to be nonessential, such that disruption of the open reading frames provides no obvious phenotype, *i.e.* LM/LAM-negative. Because disruption provided no obvious phenotype, it suggests that there are other redundant enzymes and pathways, which are able to compensate for such enzyme(s). A key goal of mycobacterial research is the generation of truncated variants of both LM and LAM. The recent definition of the Ppm1 synthase enzyme and its involvement in the extension of PIM precursors, leading to the generation of LM, has highlighted the enzyme as a worthy candidate for gene disruption leading to LM/LAM-negative mutants in mycobacteria. However, because of the intrinsic complications involved in the genetic manipulation of mycobacteria, such disruptions are likely to prove more fruitful through the initial exploitation of more tractable genetic models, such as *C. glutamicum*. Furthermore, we have found that restoration of growth rate and lipoglycan production can be observed in the *C. glutamicum*::ppm1 mutant by functional complementation with a plasmid-encoded copy of *Mt-ppm1/D2*. This finding highlights the utilization of heterologous expression of mycobacterial proteins within corynebacteria to resolve *in vivo* and *in vitro* roles of key enzymes (49, 50). As opposed to studies with *pimB* and *pimC*, further genomic and biochemical analysis established no compensatory mechanism(s) within the corynebacterial genomes, when the *Cg-ppm1* gene was inactivated.

In summary, our current findings suggest that the inactivation of *Mt-ppm1/D2* would be nonessential for *M. tuberculosis*, and provide tubercle bacilli lacking both LM and LAM. The generated mutants could then be used in detailed immunological studies aimed at defining the exact *in vivo* functions LM and LAM in tuberculosis pathogenesis. Moreover, if their *in vivo* roles are shown to echo the myriad of established *in vitro* functions, then ultimately this may lead to the development of novel agents that target this enzyme system, and as such a potential new breed of anti-mycobacterial drugs.

Acknowledgment—We gratefully acknowledge Paul Crowther for assistance with the figures.

REFERENCES

1. Kordulakova, J., Gilleron, M., Puzo, G., Brennan, P. J., Gicquel, B., Mikusova, K., and Jackson, M. (2003) *J. Biol. Chem.* **278,** 36285–36295
2. Coyle, M. B., and Lipsky, B. A. (1990) *Clin. Microbiol. Rev.* **3,** 227–246
3. Funke, G., von Graevenitz, A., Clarridge, J. E., III, and Bernard, K. A. (1997) *Clin. Microbiol. Rev.* **10,** 125–159
4. Kramer, R. (1994) *FEMS Microbiol. Rev.* **13,** 74–94
5. Stackebrandt, E., Rainey, F. A., and Ward-Rainey, N. L. (1997) *Int. J. Syst. Bacteriol.* **47,** 479–491

[4] G. S. Besra, unpublished results.

[5] L. E. DesJardin, G. S. Besra, and L. S. Schlesinger, unpublished results.

6. Eggeling, L., and Sahm, H. (2001) *J. Biosci. Bioeng.* **92,** 201–213
7. Puech, V., Chami, M., Lemassu, A., Laneelle, M. A., Schiffler, B., Gounon, P., Bayan, N., Benz, R., and Daffe, M. (2001) *Microbiology* **147,** 1365–1382
8. Brennan, P. J., and Nikaido, H. (1995) *Annu. Rev. Biochem.* **64,** 29–63
9. Sutcliffe, I. C. (1995) *Arch. Oral. Biol.* **40,** 1119–1124
10. Vercellone, A., Nigou, J., and Puzo, G. (1998) *Front. Biosci.* **3,** e149–e163
11. Nigou, J., Gilleron, M., and Puzo, G. (2003) *Biochimie* **85,** 153–166
12. Chatterjee, D., and Khoo, K. H. (1998) *Glycobiology* **8,** 113–120
13. Gilleron, M., Rivière, M., and Puzo, G. (2001) in *Glycans in Cell Interaction and Recognition: Therapeutic Aspects* (Aubery, M., ed) pp. 113–140, Harwood Academic Press, Amsterdam
14. Venisse, A., Berjeaud, J. M., Chaurand, P., Gilleron, M., and Puzo, G. (1993) *J. Biol. Chem.* **268,** 12401–12411
15. Chatterjee, D., Lowell, K., Rivoire, B., McNeil, M. R., and Brennan, P. J. (1992) *J. Biol. Chem.* **267,** 6234–6239
16. Khoo, K. H., Dell, A., Morris, H. R., Brennan, P. J., and Chatterjee, D. (1995) *J. Biol. Chem.* **270,** 12380–12389
17. Gilleron, M., Himoudi, N., Adam, O., Constant, P., Venisse, A., Riviere, M., and Puzo, G. (1997) *J. Biol. Chem.* **272,** 117–124
18. Guerardel, Y., Maes, E., Elass, E., Leroy, Y., Timmerman, P., Besra, G. S., Locht, C., Strecker, G., and Kremer, L. (2002) *J. Biol. Chem.* **277,** 30635–30648
19. Chan, J., Fan, X. D., Hunter, S. W., Brennan, P. J., and Bloom, B. R. (1991) *Infect. Immun.* **59,** 1755–1761
20. Sibley, L. D., Adams, L. B., and Krahenbuhl, J. L. (1990) *Clin. Exp. Immunol.* **80,** 141–148
21. Sibley, L. D., Hunter, S. W., Brennan, P. J., and Krahenbuhl, J. L. (1988) *Infect. Immun.* **56,** 1232–1236
22. Nigou, J., Zelle-Rieser, C., Gilleron, M., Thurnher, M., and Puzo, G. (2001) *J. Immunol.* **166,** 7477–7485
23. Knutson, K. L., Hmama, Z., Herrera-Velit, P., Rochford, R., and Reiner, N. E. (1998) *J. Biol. Chem.* **273,** 645–652
24. Means, T. K., Wang, S., Lien, E., Yoshimura, A., Golenbock, D. T., and Fenton, M. J. (1999) *J. Immunol.* **163,** 3920–3927
25. Maeda, N., Nigou, J., Herrmann, J. L., Jackson, M., Amara, A., Lagrange, P. H., Puzo, G., Gicquel, B., and Neyrolles, O. (2003) *J. Biol. Chem.* **278,** 5513–5516
26. Sidobre, S., Puzo, G., and Riviere, M. (2002) *Biochem. J.* **365,** 89–97
27. Gibson, K. J. C., Gilleron, M., Constant, P., Puzo, G., Nigou, J., and Besra, G. S. (2003) *Microbiology* **149,** 1437–1445
28. Garton, N. J., Gilleron, M., Brando, T., Dan, H. H., Giguere, S., Puzo, G., Prescott, J. F., and Sutcliffe, I. C. (2002) *J. Biol. Chem.* **277,** 31722–31733
29. Gibson, K. J. C., Gilleron, M., Constant, P., Puzo, G., Nigou, J., and Besra, G. S. (2003) *Biochem. J.* **372,** 821–829
30. Khoo, K. H., Dell, A., Morris, H. R., Brennan, P. J., and Chatterjee, D. (1995) *Glycobiology* **5,** 117–127
31. Besra, G. S., Morehouse, C. B., Rittner, C. M., Waechter, C. J., and Brennan, P. J. (1997) *J. Biol. Chem.* **272,** 18460–18466
32. Kremer, L., Gurcha, S. S., Bifani, P., Hitchen, P. G., Baulard, A., Morris, H. R., Dell, A., Brennan, P. J., and Besra, G. S. (2002) *Biochem. J.* **363,** 437–447
33. Kordulakova, J., Gilleron, M., Mikusova, K., Puzo, G., Brennan, P. J., Gicquel, B., and Jackson, M. (2002) *J. Biol. Chem.* **277,** 31335–31344
34. Schaeffer, M. L., Khoo, K. H., Besra, G. S., Chatterjee, D., Brennan, P. J., Belisle, J. T., and Inamine, J. M. (1999) *J. Biol. Chem.* **274,** 31625–31631
35. Gurcha, S. S., Baulard, A. R., Kremer, L., Locht, C., Moody, D. B., Muhlecker, W., Costello, C. E., Crick, D. C., Brennan, P. J., and Besra, G. S. (2002) *Biochem. J.* **365,** 441–450
36. Keilhauer, C., Eggeling, L., and Sahm, H. (1993) *J. Bacteriol.* **175,** 5595–5603
37. Schafer, A., Tauch, A., Jager, W., Kalinowski, J., Thierbach, G., and Puhler, A. (1994) *Gene* (*Amst.*) **145,** 69–73
38. Jakoby, M., and Burkovski, A. (1999) *Biotechnol. Techniques* **13,** 437–441
39. Link, A. J., Phillips, D., and Church, G. M. (1997) *J. Bacteriol.* **179,** 6228–6237
40. Hunter, S. W., and Brennan, P. J. (1990) *J. Biol. Chem.* **265,** 9272–9279
41. Westphal, O., and Jann, K. (1965) in *Methods in Carbohydrate Chemistry* (Whistler, R. L., ed) pp. 83–91, Academic Press, Orlando, FL
42. Ciucanu, I., and Kerek, F. (1984) *Carbohydr. Res.* **131,** 209–217
43. Baulard, A. R., Gurcha, S. S., Engohang-Ndong, J., Gouffi, K., Locht, C., and Besra, G. S. (2003) *J. Biol. Chem.* **278,** 2242–2248
44. Pitulle, C., Dorsch, M., Kazda, J., Wolters, J., and Stackebrandt, E. (1992) *Int. J. Syst. Bacteriol.* **42,** 337–343
45. Orlean, P., Albright, C., and Robbins, P. W. (1988) *J. Biol. Chem.* **263,** 17499–17507
46. Gilleron, M., Ronet, C., Mempel, M., Monsarrat, B., Gachelin, G., and Puzo, G. (2001) *J. Biol. Chem.* **276,** 34896–34904
47. Gilleron, M., Quesniaux, V. F., and Puzo, G. (2003) *J. Biol. Chem.* **278,** 29880–29889
48. Fratti, R. A., Chua, J., Vergne, I., and Deretic, V. (2003) *Proc. Natl. Acad. Sci. U. S. A.* **100,** 5437–5442
49. Salim, K., Haedens, V., Content, J., Leblon, G., and Huygen, K. (1997) *Appl. Environ. Microbiol.* **63,** 4392–4400
50. Puech, V., Bayan, N., Salim, K., Leblon, G., and Daffe, M. (2000) *Mol. Microbiol.* **35,** 1026–1041